Appl Phys B (2009) 96: 309–314
DOI 10.1007/s00340-008-3355-1

Applied Physics B
Lasers and Optics

Ultrashort pulse electron gun with a MHz repetition rate

D. Wytrykus · M. Centurion · P. Reckenthaeler · F. Krausz · A. Apolonski · E. Fill

Received: 5 December 2008 / Published online: 23 January 2009

Abstract We report the construction of an electron gun emitting ultrashort pulses with a repetition rate of 2.7 MHz. The gun works at an acceleration voltage of 20 kV and is operated with a laser oscillator having an ultralong cavity. A low number of electrons per pulse eliminates space charge broadening. Electron yield and beam profiles are measured for operation with laser wavelengths of 800, 400, and 266 nm. The initial energy spread of the electrons is determined for these three wavelengths, and pulse durations of 600, 390, and 270 fs are inferred from the data.

PACS 87.15.Aa · 87.59.-e · 61.10.-i

1 Introduction

Ultrafast electron diffraction (UED) has become a powerful tool in the investigation of ps and sub-ps processes in molecules and solids. Examples of such studies include photo-dissociation of molecules [1], detection of fast photo-induced conformational changes [1–3], and ultrafast phase changes in solids [4, 5].

Unfortunately, however, the mutual repulsion of the electrons prevents the generation of electron pulses as short as the femtosecond laser pulse releasing the electrons from the photocathode. This so-called space charge broadening limits the temporal resolution of UED at present to about 300 fs. Several methods have been used or proposed to generate ultrashort electron pulses in spite of space charge broadening. These include using a very short electron gun [2], applying relativistic electrons [6], and generating an energy chirp to focus temporally the electrons by means of a "temporal lens" [7] or by acceleration through an RF-cavity [8–10]. Yet another approach to eliminate space charge broadening is based on reducing the pulse charge to one or a few electrons per pulse. To keep acquisition times at a tolerable level, the repetition rate of the pulses must be accordingly increased [11]. In this paper we report the realization of an electron gun operated by a laser with a 2.7 MHz repetition rate and with a very low charge of up to two electrons per pulse [12].

2 Experiment

2.1 Experimental setup

The experimental setup is schematically sketched in Fig. 1. The gun consists of two chambers connected by a drift tube (Fig. 1a). The first chamber houses the acceleration stage consisting of HV-feedthrough cathode and anode. A fused silica window allows the laser pulse to be focused onto the cathode. The other chamber contains the detector. A quartz plate coated with a 50-nm layer of gold was used as the cathode. The acceleration voltage of 20 kV was supplied to the cathode by means of a brass ring pressed against the outer part of it (Fig. 1b). For the anode either a 1-cm-thick copper disk with a hole 1 mm in diameter or, alternatively, a thin metal net with a mesh size of 83 μm was used. The detector

D. Wytrykus · P. Reckenthaeler · F. Krausz · A. Apolonski · E. Fill (✉)
Ludwig-Maximilians-Universität München, Am Coulombwall 1, 85748 Garching, Germany
e-mail: ernst.fill@mpq.mpg.de
Fax: +49-89-28914141

M. Centurion · P. Reckenthaeler · F. Krausz · E. Fill
Max-Planck-Institut für Quantenoptik, Hans-Kopfermann-Str. 1, 85748 Garching, Germany

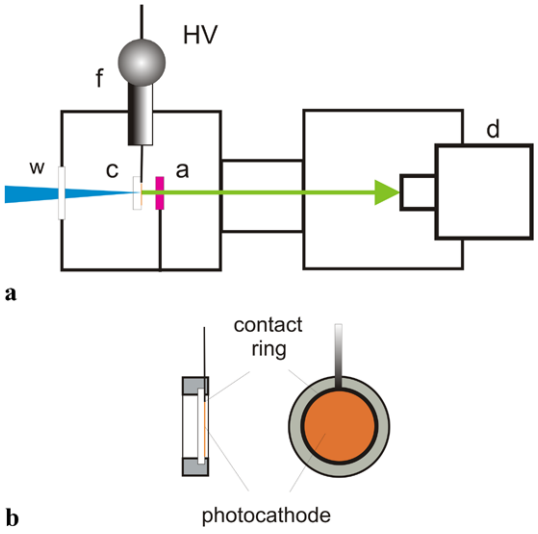

Fig. 1 **a** Basic layout of the electron gun. w: window for trigger laser; c: cathode holder; a: anode; f: high-voltage feedthrough, d: detector with sensitized fiber extension. The edge length of the two cubes is 20 cm, the length of the drift tube is 10 cm. The distance from the anode to the detector was 30 cm. **b** Detailed drawing of the cathode assembly in side and front view

consisted of a CCD with a 1:1 cylindrical fiber plate, made sensitive for electrons by coating it with phosphor P43.

The laser used for operating the electron gun has been described elsewhere [13]. In short, it is a Kerr-lens-mode-locked fsec titanium:sapphire chirped-pulse oscillator operated with a net positive intracavity group delay dispersion. Under these conditions, the oscillator generates a train of broadband chirped pulses with ≈2 ps duration. Two intracavity Herriott delay lines increased the cavity roundtrip path length to 111 m, resulting in a repetition rate of 2.7 MHz. An extracavity dispersive delay line consisting of chirped mirrors compresses the pulses to ≈50 fs (FWHM). The maximum pulse energy after compression is 230 nJ.

The electron gun was operated with the fundamental, the second harmonic, and the third harmonic of the titanium sapphire laser output. The laser pulses were focused onto the cathode by a 300 mm focal length lens. The peak intensity at the fundamental was 3×10^{10} W/cm^2. The second harmonic was generated by focusing the laser with a 75-mm focal-length lens into a 0.3-mm-long beta barium borate crystal (BBO). A conversion efficiency of 4% was measured. The third harmonic was generated by placing in the same focus another BBO crystal with a length of 0.3 mm for fundamental-second harmonic sum-frequency generation. Insertion of a polarization rotation and a delay plate was not possible because of the short focus. Nevertheless a conversion efficiency of 5×10^{-4} into the third harmonic was achieved.

2.2 Measurements

The number of electrons per pulse was measured by calibrating the detector in a different electron gun by means of a Faraday cup (Kimball Physics, model FC-70C) coupled to a pico-Amperemeter (Keithley, model 480). In the MHz gun the highest beam current was 0.8 pA, measured with a fundamental laser power of 650 mW on the cathode. This corresponds to about 2 electrons per pulse at a 2.7 MHz repetition rate.

The work function of gold in a thin layer was found to be reduced to 4.5 eV [14] in contrast to the literature value of 5.1 eV for bulk polycrystalline material [15]. For a titanium sapphire laser (fundamental photon energy $h\nu = 1.55$ eV), one would expect that one, two, and three photons are required for emitting an electron with the third harmonic, second harmonic, and fundamental, respectively. The measurements of beam current vs. laser intensity confirm this assumption except for the fundamental. Figures 2a–c show the beam current vs. laser power for the three wavelengths. In these experiments the laser was focused to a spot 140 µm in diameter by a 30-cm focal-length lens. The double logarithmic display of the data allows a correlation with the power of the multiphoton effect to be made. It turns out that for the second and third harmonics, the expected slope 2 and slope 1 dependences are obtained, but somewhat surprisingly, for the fundamental, a slope 5.3 dependence was fitted. This may be due to the relatively high intensity which leads to an emission analogous to above-threshold-ionization of atoms (ATI).

The minimum pulse duration of an electron gun without space charge broadening is limited by the initial energy spread of the electrons emitted from the cathode. Without space charge broadening the pulse duration resulting from the initial energy of the electrons is given by [16]

$$\tau_p(s) = 2.34 \times 10^{-12} (\varepsilon_{\mathrm{el}})^{1/2} / E_{\mathrm{acc}}. \quad (1)$$

In this equation $\varepsilon_{\mathrm{el}}$ is the initial electron energy spread of the electrons in eV, and E_{acc} is the acceleration field in kV/mm. In the following we show that the initial energy spread can be determined from the profile of the electron beam on the detector.

For this purpose, the solid copper anode was replaced by a metal wire-grid with a mesh size of 83 µm. In this way a very homogeneous field was generated in the acceleration stage. Figure 3 shows electron beam profiles on the detector for different laser wavelengths with the mesh anode in place. For fundamental and second harmonic irradiation, the mesh shows up in the electron beam pattern indicating that the beam emitted from the cathode spreads significantly in lateral direction. For the third harmonic, the mesh is not visible in the electron beam profile. This is due to the fact that the small beam diameter of the UV light (less than 1 mm)

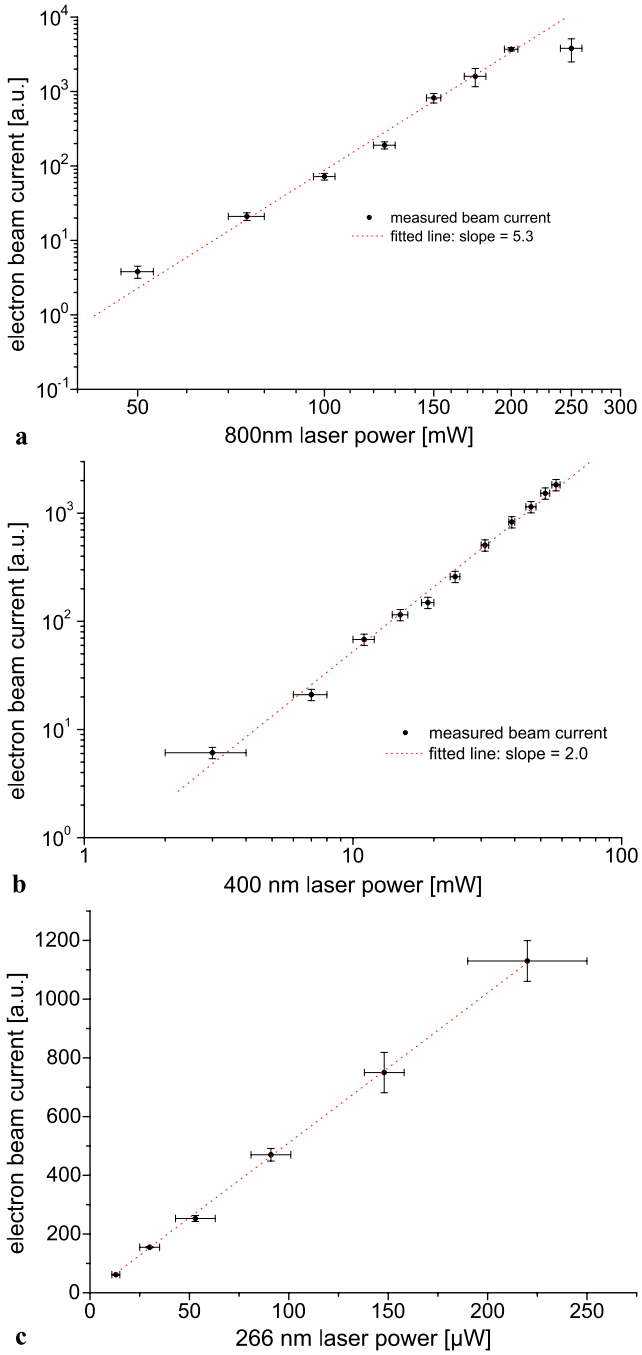

Fig. 2 **a** Electron beam current vs. fundamental laser power. The data are fitted with a power law with slope 5.3 indicating above threshold emission. **b** Electron beam current vs. laser power for 400-nm laser light (second harmonic). A power law with a power of two describes the dependence. **c** Electron beam current vs. third harmonic laser power. A linear correlation is obtained

resulted in a relatively large spot on the cathode, and thus the mesh pattern is washed out.

It is interesting to observe that the mesh wires show up as bright bars in the image and not as dark lines as in a simple shadowgram. This is due to the fact that the electric field

Table 1 Electron energy spread and electron distribution after photoemission with fundamental, second, and third harmonic laser light

Laser wavelength	Function of electron spectrum	$\varepsilon_{\mathrm{el}}$ (eV)
800 nm	Exponential	0.6
400 nm	Exponential	0.25
266 nm	Gaussian	0.12

penetrates slightly through the mesh loops, and thus the bars act as positively charged wires for the electrons. The electron traces are therefore slightly bent around the mesh bars resulting in an increased intensity on the detector.

To derive the initial electron energy from the beam profile, the distribution $f(\upsilon_t)$ of transverse velocities υ_t for a given distribution $f(\upsilon)$ of absolute velocities υ has to be calculated. In the Appendix the relation

$$f(\upsilon_t) = C \int_{\upsilon_t}^{\infty} d\upsilon \frac{f(\upsilon)}{\sqrt{\upsilon^2 - \upsilon_t^2}} \tag{2}$$

is derived (4), where C is a constant.

To map transverse velocities to a beam profile, one needs a relation between the transverse velocity of an electron and its distance ρ from the beam axis at the detector. Denoting the lengths of the acceleration and drift regions by L_a and L_d, one obtains

$$\rho = (2L_a + L_d)\frac{\upsilon_t}{\upsilon_{\mathrm{long}}}, \tag{3}$$

where υ_{long} is the longitudinal velocity after acceleration. In υ_{long} the small difference in velocities resulting from the initial electron velocity spread can be safely neglected. Note that (3) is derived nonrelativistically. The acceleration distance L_a has to be counted twice in the equation since the time of an electron spent in the acceleration stage is exactly twice the time needed for traversing it with the final velocity.

Equations (2) and (3) now enable us to calculate the beam pattern resulting from a given velocity distribution. For this purpose, (2) is solved numerically, and then the intensity profile on the detector is calculated using (3). Exponential and Gaussian energy distributions $f_e(E) \propto \exp(-E/\varepsilon_{\mathrm{el}})$ and $f_g(E) \propto \exp(-E^2/2\varepsilon_{\mathrm{el}}^2)$ with $f(\upsilon)d\upsilon = f(E)\, m\upsilon\, d\upsilon$ were fitted to the data (m is the electron mass). The results are given in Table 1. We note that the result for the third harmonic of an initial energy spread of 0.12 eV is in good agreement with the value of 95 meV obtained with electron spectrometry [14]. No previous data are available for the other laser wavelengths.

The data in the table allow estimating the pulse durations under the different conditions of irradiation by using (1). With an end vacuum of 10^{-5} mbar in our apparatus, the maximum electric field that could be reliably sustained in

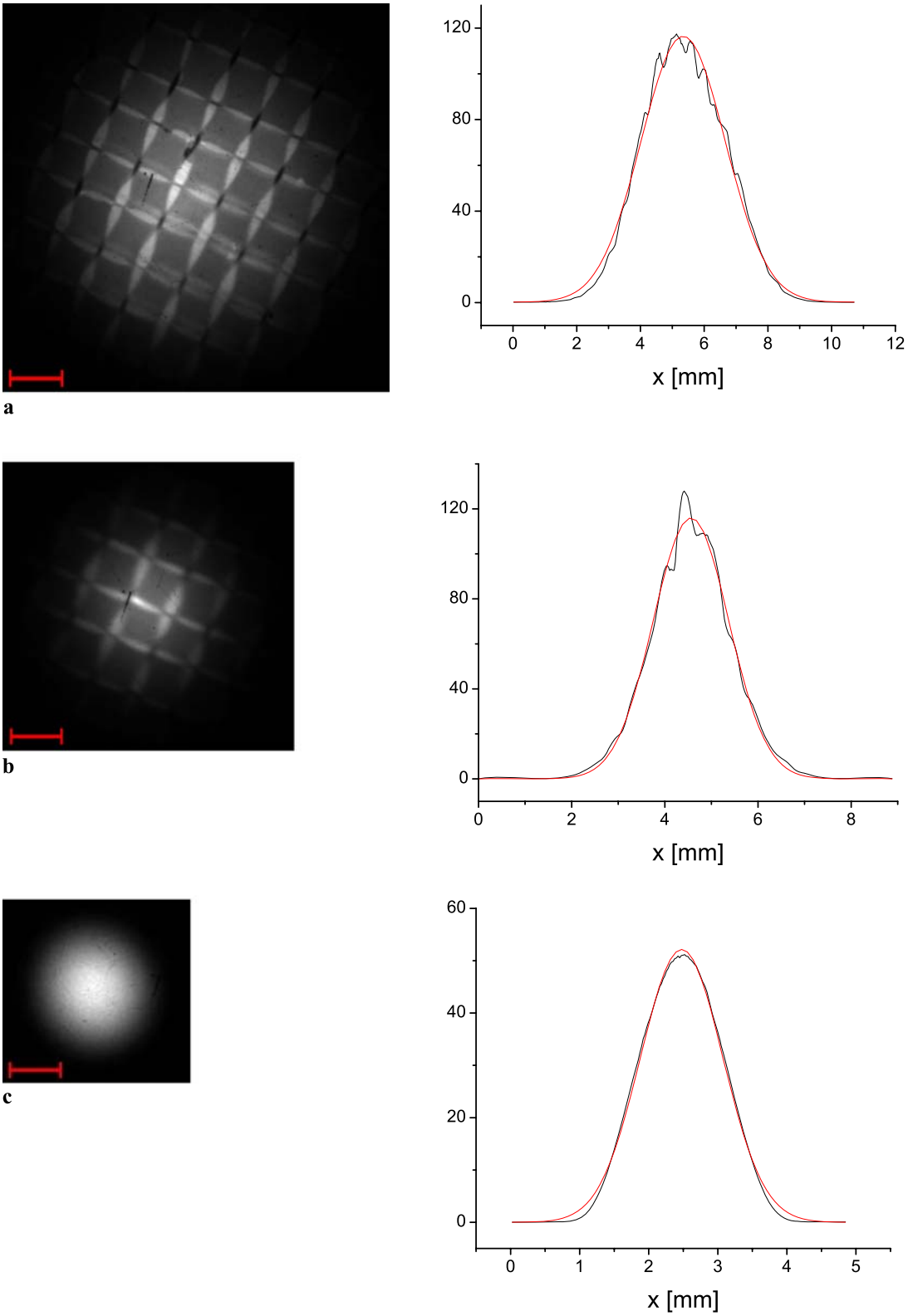

Fig. 3 Beam patterns and profiles with the mesh anode in place. Line outs and Gaussian fits are shown. The *red bars* indicate a distance of 1 mm on the detector. **a** Beam pattern and profile for illumination of cathode with fundamental; **b** with second harmonic; **c** with third harmonic light

the acceleration gap was 3 kV/mm. The corresponding pulse durations are 600, 390, and 270 fs for photoemission with fundamental, second harmonic, and third harmonic laser light. Under UHV conditions, fields of 10 kV/mm have been reported to be applicable before vacuum breakdown occurs [17]. With such a high acceleration field, generation of pulses with durations of less than 100 fs seems feasible. The additional possibility of temporal focusing by means of an electron energy chirp generated by an RF-cavity will allow advancing into the few-fs or even as-region [7–10].

3 Conclusions

A simple electron gun was operated with a repetition rate of 2.7 MHz, as predetermined by the laser. The number of electrons was varied between about 10^{-4} and two per pulse by varying the intensity of the laser. The gun was operated with the fundamental, second harmonic, and third harmonic of the laser. The corresponding multi-photon effects resulted in power laws for the beam current vs. laser power dependence. With a fine mesh as the anode, evaluation of the beam profile allowed determining the initial energy spread of the electrons. An analysis of the data yields an energy spread of 0.12 eV for third harmonic light illumination resulting in a pulse duration of 270 fs.

With this system—combined with an additional laser amplifier to boost the pulse energy into the 10-μJ region—a technique has been demonstrated which is capable of performing UED pump-probe experiments with fs-electron pulses at a MHz repetition rate.

Appendix: Derivation of (2)

We start from the most general case of a two-parameter distribution $f(\upsilon, \Theta)$ of velocities and angles. To obtain $f(\upsilon_t)$ one has to integrate $f(\upsilon, \Theta)$ over all possible velocities υ and angles Θ that yield υ_t, subject to the relation $\upsilon_t = \upsilon \sin \Theta$, i.e.,

$$f(\upsilon_t) = \int_0^{\pi/2} d\Theta \int_{\upsilon_t}^{\infty} d\upsilon\, f(\upsilon, \Theta)\delta(\upsilon_t - \upsilon \sin\Theta). \tag{4}$$

The lower boundary of the second integral is υ_t since the length of the velocity vector must at least be υ_t. To get rid of the delta function and perform the integration over Θ, we use the generalized scaling theorem of the delta function (see, e.g., http://en.wikipedia.org/wiki/Dirac_delta_function) to obtain

$$f(\upsilon_t) = \int_{\upsilon_t}^{\infty} d\upsilon \frac{f(\upsilon, \Theta)}{\upsilon \cos\Theta} = \int_{\upsilon_t}^{\infty} d\upsilon \frac{f(\upsilon, \Theta)}{\sqrt{\upsilon^2 - \upsilon_t^2}}, \tag{5}$$

where use has been made of $\Theta = \arcsin(\upsilon_t/\upsilon)$.

The angular distribution of the emitted electrons has now to be specified. We make the ansatz of an isotropic emission into half-space, a reasonable assumption for a polycrystalline material. Thus $f(\upsilon, \Theta) = Cf(\upsilon)$, and (5) simplifies to

$$f(\upsilon_t) = C \int_{\upsilon_t}^{\infty} d\upsilon \frac{f(\upsilon)}{\sqrt{\upsilon^2 - \upsilon_t^2}}, \tag{6}$$

where C is a constant. Normalization of the distribution is not required since we are only interested in the shape of the electron beam profile, not its intensity.

Acknowledgements This work was funded in part by Deutsche Forschungsgemeinschaft (DFG) under contract SFB Transregio 6039 and by the DFG Cluster of Excellence "Munich Centre for Advanced Photonics" (MAP; www.munich.photonics.de). M.C. was supported by a research fellowship from the Alexander von Humboldt foundation. P.R. is supported by a scholarship from the International Max-Planck Research School on Advanced Photon Science (IMPRS-APS; www.mpq.mpg.de/APS).

References

1. M. Dantus, S.B. Kim, J.C. Williamson, A.H. Zewail, J. Phys. Chem. **98**, 2782–2796 (1994)
2. J.R. Dwyer, C.T. Hebeisen, R. Ernstorfer, M. Harb, V.B. Deyirmenjian, R.E. Jordan, R.J. Dwayne Miller, Philos. Trans. R. Soc. A **364**, 741–778 (2006)
3. H. Ihee, V.A. Lobastov, U.M. Gomez, B.M. Goodson, R. Srinivasan, C.-Y. Ruan, A.H. Zewail, Science **291**, 458–462 (2001)
4. P. Baum, A.H. Zewail, Proc. Natl. Akad. Sci. **103**, 16105–16110 (2006)
5. B.J. Siwick, J.R. Dwyer, R.E. Jordan, R.J. Dwayne Miller, Science **302**, 1382–1385 (2003)
6. J.B. Hastings, F.M. Rudakov, D.H. Dowell, J.F. Schmerge, J.D. Cardoza, J.M. Castro, S.M. Gierman, H. Loos, P.M. Weber, Appl. Phys. Lett. **89**, 184109 (2006)
7. M. Monastyrskiy, S. Andreev, D. Greenfield, G. Bryukhnevich, V. Tarasov, M. Schelev, in *High-Speed Photography and Photonics*, vol. 5580 (SPIE, Bellingham, 2005), pp. 324–334
8. E. Fill, L. Veisz, A. Apolonski, F. Krausz, New J. Phys. **8**, 272 (2006)
9. S.B. van der Geer, M.J. de Loos, T. van Oudheusden, W.P.E.M. Op't Root, M.J. van der Wiel, O.J. Luiten, Phys. Rev. Spec. Top., Accel. Beams **9**, 044203 (2006)
10. L. Veisz, G. Kurkin, K. Chernov, V. Tarnetsky, A. Apolonski, F. Krausz, E. Fill, New J. Phys. **9**, 451–457 (2007)
11. V.A. Lobastov, R. Srinivasan, A.H. Zewail, Proc. Natl. Akad. Sci. **102**, 7069–7073 (2005)
12. D. Wytrykus, *Design and Characterization of a Source of Ultrashort Electron Pulses at a MHz Repetition Rate* (University of Munich, Munich, 2008), pp. 1–76

13. S. Naumov, A. Fernandez, R. Graf, P. Dombi, F. Krausz, A. Apolonski, New J. Phys. **7**, 216 (2005)
14. A. Janzen, B. Krenzer, O. Heinz, P. Zhou, D. Thien, A. Hanisch, F.-J. Meyer zu Heringdorf, D. von der Linde, M. Horn von Hoegen, Rev. Sci. Instrum. **78**, 013906 (2007)
15. H.B. Michaelson, J. Appl. Phys. **48**, 4729–4733 (1977)
16. M.Y. Schelev, M.C. Richardson, A.J. Alcock, Appl. Phys. Lett. **18**, 354–357 (1971)
17. B.J. Siwick, J.R. Dwyer, R.E. Jordan, R.J. Dwayne Miller, Chem. Phys. **299**, 285–305 (2004)